Journal of Applied Electrochemistry (2005) 35:405–411
DOI 10.1007/s10800-005-0799-4

Deactivation and regeneration of Pt anodes for the electro-oxidation of phenol

D. FINO*, C. CARLESI JARA, G. SARACCO, V. SPECCHIA and P. SPINELLI
Materials Science and Chemical Engineering Department, Politecnico di Torino, Corso Duca degli Abruzzi, 24, 10129 Torino, Italy
*(*author for correspondence, e-mail: debora.fino@polito.it; phone: +39-011-5644710; fax: +39-011-5644699)*

Received 18 March 2004; accepted in revised form 15 December 2004

Key words: activated carbon, anode, deactivation, electro-oxidation, PbO_2, phenol, Pt, regeneration, $Ti/IrO_2/Ta_2O_5$, voltammetry

Abstract

Electro-oxidation tests with different electrolytes (Na_2SO_4, NaCl, H_2SO_4) and anode types (Pt, Ti lined with Ir and Ta oxides, PbO_2, activated carbon) were performed on aqueous solutions containing phenol to assess the mechanism and nature of electrode deactivation phenomena. For the Pt electrode, the nature of the electro-deposited organic species was investigated by ATR-FTIR and FESEM-EDS analyses, which showed adsorption of intermediate oxidation products (e.g. benzoquinone, hydroquinone) is likely responsible for the early deactivation stages. Conversely, in the longer term, formation of polymeric films is promoted. Potentiostatic tests showed that anode regeneration can be achieved by anodic polarisation above 1.1 V (vs Hg/Hg_2SO_4). This reactivation was found to be easier in the presence of significant amounts of chloride ions. Conversely, the deactivated state is maintained for the $Ti/IrO_2/Ta_2O_5$ electrode even though anodic polarisation at high positive potentials is applied. Cyclic voltammetric curves on PbO_2 electrodes did not provide satisfactory results as the intensity of the lead-dioxide reduction peak was so high that peaks for phenol oxidation were hardly detectable. Finally, the activated carbon based electrode was found to be promising as it enables simultaneous adsorption of the organic pollutant and oxidation of the pollutant itself to constitute a sort of self-regenerating adsorber unit.

1. Introduction

The electrochemical oxidation of organic pollutants is a promising treatment for substances which are recalcitrant to biological degradation, i.e. the cheapest and most widespread technology to abate organics from domestic and industrial effluents.

In previous investigations performed on a divided electrolytic cell equipped with a Pt–Ti anode [1, 2], it has been shown that, when working at sufficiently low electrolyte concentrations (≤ 0.01 M Na_2SO_4 or ≤ 0.02 M NaCl) to enable direct discharge of the waste water into water basins according to Italian law (DL 152 /11-5-99), high electrode potentials have to be adopted to achieve significant pollutant conversion per unit electrode surface. These operating conditions entail the formation of bulk oxidants. As a consequence, two oxidation processes must be considered: the first depends on the production of bulk oxidants (e.g. H_2O_2, persulphates, hypochloric acid), the second on the OH° radicals which are generated at the anode. Particularly, in sulphate-rich media it is likely that the H_2O_2 is formed by hydrolysis of persulphates from anodic oxidation of anions [2]. Conversely, in the presence of chlorides, electrochemical oxidation routes involving the formation of bulk ClO^- are likely [3].

Furthermore, it has been demonstrated that ferrous ions promote bulk oxidation processes taking place in the electrolyte, especially at the low pH values established in the anodic compartment [3, 4]. Chlorides were also found to accelerate the electrochemical degradation of organics more than sulphates [3], at the cost of producing chlorinated hydrocarbons as reaction intermediates. When PbO_2 anodes are used, the effect of bulk oxidation is limited because lead dioxide is less active than Pt–Ti in the promotion of H_2O_2 formation. However, PbO_2 electrodes enable high TOC abatement, as a consequence of comparatively faster direct oxidation pathways [4].

The process of direct anodic oxidation of phenol involves various steps: after adsorption on the anode, phenol is oxidised to form a radical [5], that can be further oxidised to hydroquinone and then to benzoquinone or can react to form a polymeric structure less reactive than the phenol and characterised by strong adhesion to the electrode surface. This last occurrence entails electrode deactivation and hinders further oxidation of phenol. Some SEM observations of the fouling layers [6] suggest that, after oxygen evolution, small

blisters form in the layers causing the generation of uncovered areas of the electrode surface.

Anodic oxidation of phenol has been the subject of fundamental [7–9] and applied [10, 11] studies. Various anode materials have been studied including Pt, Ti covered with oxides, lead dioxide and boron-doped diamond. In the absence of chlorides the main oxidation products are benzoquinone and hydroquinone with some traces of cathecol and carboxilic acids. In the presence of chlorides [12] with IrO_2–Ti and SnO_2–Ti, electro-generated ClO^- should play an active role in the oxidation process, leading to the formation of organic chlorinated compounds, which may be further oxidised to volatile organic compounds (e.g. $CHCl_3$).

In the present work, the oxidation of phenol on various anodes is addressed with special focus on the electrode deactivation phenomena which are known to progressively reduce the treatment efficiency. In the case of the Pt anode, the investigation is expanded to assess the effect of the nature of the electrolyte (sulphates, chlorides) and of its concentration, in view of the direct discharge of waste waters into water basins.

2. Experimental

The cell used in the present investigation was undivided and consisted of a glass open vessel kept at constant temperature (normally 25 ± 0.2 °C). Some specific runs were also carried out at different temperatures in the range 20–30 °C. Different anodes were tested: a Pt foil, a Ti–Ir–Ta_2O_5 rod, PbO_2 formed on an Au sheet, and a layer of active carbon (Norit R2510/AFO-1320) pressed on a Pt current collector. A Pt foil was used as the counter electrode. The electrode potentials were measured with reference to a Hg–$HgSO_4$ electrode. The reference electrode was set at small distance from the working electrode surface in order to minimise errors. The surface area of the electrodes was 4 cm^2. The cell was connected to a VoltaLab® electrochemical system controlled by a PC which permitted the automatic acquisition of electrical parameters i.e. the electrode potential (E) and the current density (j). All the treated solutions were prepared using analytical grade chemicals and tri-distilled water.

The tests were carried out both in potentiodynamic and in galvanostatic conditions. The reaction progress was followed by small anolyte samples withdrawal for spectrophotometric (Unicam UV2, double ray) and HPLC (Varian Pro Star double pump HPLC equipped with UV–VIS diode array detector, DAD, and a Chrompack chromatographic column: Lichrospher 5RP18 SS 250 × 4.6 mm) analyses. Chlorinated compounds were instead analysed by mass spectrometry (Gaschromatograph Varian 3800 with MS/MS Saturn 2000 mass spectrometer, Chrompack CP WAX 52CB 60 m column and 1 ml min^{-1} He carrier) after extraction with di-chloro methane. As regards the carbon electrodes, the analysis of the products adsorbed was performed using the method proposed in [8].

The Pt electrode was polished before the tests according to an electrolytic treatment in 30-wt% HNO_3 (galvanostatic polarisation at −360 and 360 mA) followed by 10 voltammetric cycles (100 mV s^{-1}) in 1 M sulphuric acid between −700 and 1200 mV vs Hg/Hg_2SO_4. The Ti/IrO_2/Ta_2O_5 electrode was polished with Fenton reagent, whereas the PbO_2 and the carbon electrodes were prepared freshly for each test. Before tracing the voltammetric $j(E)$ curves, all electrodes underwent 10 cycles in a basic organic-free solution as a common pre-treatment.

Further analyses were performed on the clean and deactivated Pt electrodes by:

- Attenuated Total Reflectance (ATR)-FTIR spectroscopy (Bruker IFS 55 Equinox instrument equipped with a MCT cryodetector). The ATR equipment allows FTIR spectra of poorly transmitting samples to be collected and is suitable for detection of organic molecules present on the electrode surface in either adsorbed or polymerised form;
- Field Emission Scanning Electrode Microscopy (FESEM - Leo 50/50 VP with GEMINI column) with EDS detector. The FESEM–EDS combination allows both the morphology and the elemental composition of the electrode deactivating layers to be determined.

3. Results and discussion

Typical voltammograms for phenol (Ph) oxidation on Pt in sulphuric acid are shown in Figure 1a. The anodic part of the two first cycles indicates the electrode deactivation. This is in line with earlier workers [5, 14], who attributed this phenomenon to surface fouling by an adherent film generated by polymerisation of phenoxy radicals produced in the oxidation.

The influence of the phenol concentration (Figure 1b) and the typical triangular trend of the voltammograms suggest that the early deactivation occurs through the adsorption of the anodic products on the electrode active sites. The higher the phenol concentration the lower the electrode potential at which oxidation is promoted, but the lower the potential at which deactivation occurs. Furthermore, the higher the phenol concentration, the lower the area of the voltammograms. High phenol concentrations accelerate the anodic oxidation process, and also the production of partially oxidised products which are readily adsorbed on the electrode surface.

The data collected at different operating temperatures (Figure 1c) confirm that the crucial deactivation process should actually be adsorption of reaction intermediates. An increase in temperature reduces physical adsorption, but also favours decomposition and desorption of chemically adsorbed species. Both possibilities explain the increase in the voltammogram peak area as a

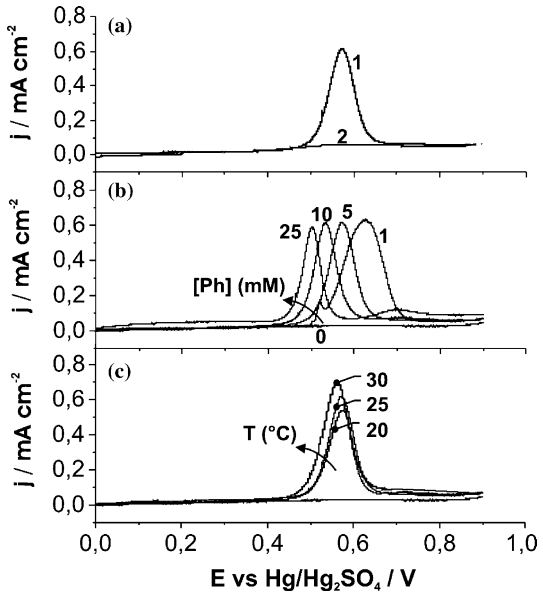

Fig. 1. Anodic part of voltammetric curves for phenol oxidation in 0.5 M H_2SO_4 on a Pt-anode (initial potential = 0 V, sweep rate = 10 mV s^{-1}): [Ph] = 5 mM, T = 25 °C, curve 1 the first cycle, curve 2 the second cycle. Influence of Ph concentration at 25 °C. Effect of operating temperature on voltammetric curves for [Ph] = 5 mM.

function of temperature. If a rapid polymerisation process occurred, temperature would probably have promoted deactivation, by accelerating the kinetics of the polymerisation process.

Although the electrochemistry of phenols is complex [15, 16], it may be argued that adsorption of intermediates leads to immediate deactivation (after the first voltammetric cycle), whereas the formation of a polymer film covering the electrode occurs in the long term on the grounds of comparatively slower kinetics. This is confirmed by the ATR–FTIR spectrum for the Pt electrode deactivated after a single voltammetric cycle (Figure 2). On the grounds of the NIST spectra database [17] the absorbance peaks detected in Figure 2 can be easily related to: hydroquinone (3251, 2880, 1441, 1153 cm^{-1}), benzoquinone (1764, 1310, 1032, 874 cm^{-1}) and unreacted phenol (3376, 1631, 1441, 1153 cm^{-1}).

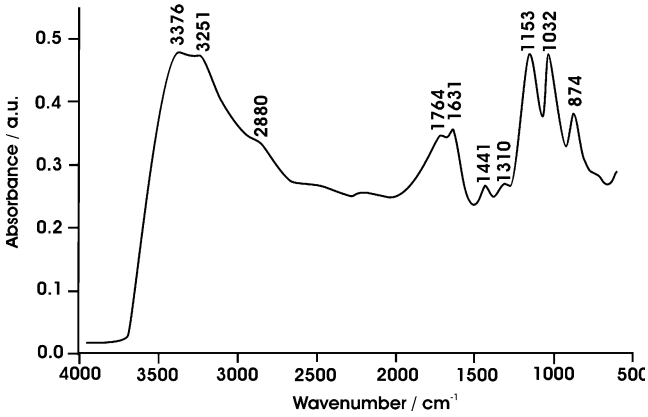

Fig. 2. ATR-FTIR spectrum of the Pt electrode deactivated after a single voltammteric cycle.

Figure 3 shows the FESEM micrographs of a clean and a heavily deactivated (24 h operation at +0.7 V under 5 mM Ph) Pt-electrode surface. The growth of an irregular and blistered polymer layer over the electrode surface is evident. Elemental analysis at a blistered location (see the highlighted area on the right picture of Figure 3) showed that even where the direct presence of the polymer layer is not evident, a significant amount of carbon and oxygen is present over the electrode surface, as opposed to the clean electrodes (see Figure 3 caption). The listed elemental weight percentages correspond to an average C:O atomic ratio of about 4, higher than the ratio of such elements in the hydroquinone or benzoquinone structures (C:O = 3) but lower than that of phenol or of polymer molecules obtained by poly condensation (C:O = 6). This suggests the co-existence of all these molecules on the deactivated electrode surface.

Such deactivation can be partially eliminated if the electrode is polarised at high positive potential. This effect cannot be simply ascribed to the mechanical effect of gas bubbles evolving at the electrode surface, because the breakdown of the fouling layer is not observed to a significant extent when the electrode, after deactivation,

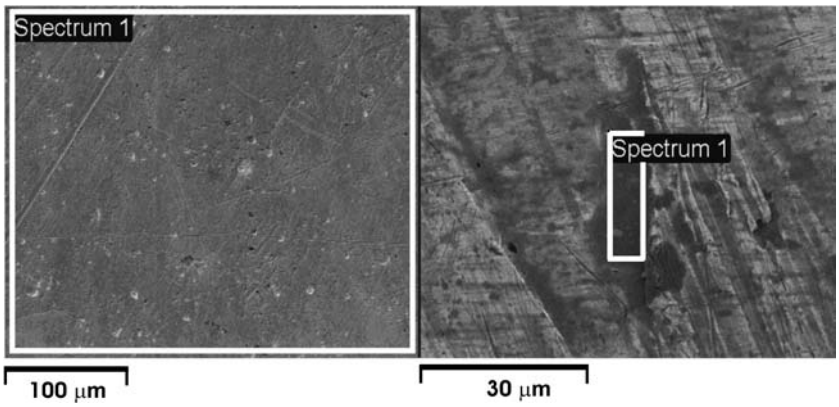

Fig. 3. FESEM pictures of a clean (left) and heavily fouled (right) Pt electrode. Average elemental composition data derived by EDS analysis over the indicated spectrum areas (weight %): (clean electrode) C = 0.42%, Pt = 99.58%; (deactivated electrode) C = 19.68 %, O = 6.54% Pt = 73.77%.

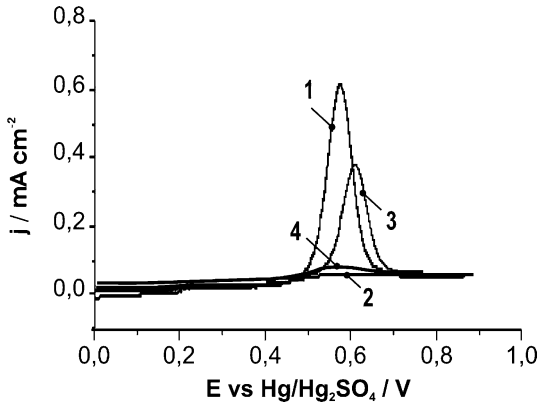

Fig. 4. Anodic part of voltammetric curves for phenol oxidation over the Pt electrode in clean state (1), after deactivation (2), and after reactivation for 15 min both at +1500 mV (3) and −800 mV (4). Experimental conditions: [Ph] = 5 mM in 0.5 M H_2SO_4, T = 25 °C; initial potential = 0 V, sweep rate = 10 mV s^{-1}.

is cathodically polarised in the range of hydrogen evolution, as shown in Figure 4. In this figure, four voltammograms are reported: for the clean electrode, for the deactivated one and for the electrode maintained at high positive (1500 mV vs Hg/Hg_2SO_4, inducing O_2 formation) or negative potential (−800 mV vs Hg/Hg_2SO_4, inducing H_2 formation). One might think that the electrode re-activation is due to oxidation due to the $OH^{\cdot}$ radical produced on the anode. This radical can partially oxidise the adsorbed intermediates or even the polymeric layer eventually formed, thereby uncovering some active sites for phenol adsorption and reaction. This effect should depend on the applied potential (Figure 5a) and on the time of the reactivation treatment (Figure 5b) as such parameters directly influence the $OH^{\cdot}$ production and the extension of uncovered areas, respectively. After a regeneration treatment by application of a +1500 mV over-potential for 10 min

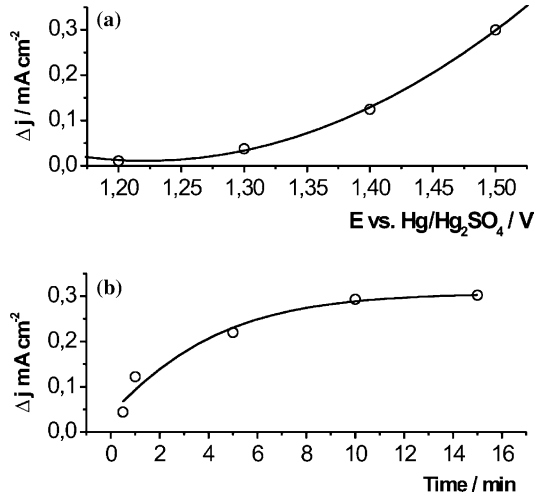

Fig. 5. Influence of reactivation potential (a: after 15 min) and time (b: at 1500 mV) on recovery peak intensity for 5 mM phenol in 0.5 M H_2SO_4 over a Pt anode (initial potential = 0 V, sweep rate = 10 mV s^{-1}).

Table 1. Formation potential of several bulk oxidants

Oxidant	Formation Potential (V) vs NHG
Hydroxyl radical (H_2O/OH)	2.80
Ozone (O_2/O_3)	2.07
Peroxodisulfate ($SO_4^{2-}S_2O_8^{2-}$)	2.01
Hydrogen peroxide (H_2O/H_2O_2)	1.77
Chlorine dioxide (Cl^-/ClO_2^-)	1.57
Chlorine (CL^-/Cl_2)	1.36
Oxygen (H_2O/O_2)	1.23

the average percentage of carbon over the Pt surface of the heavily deactivated electrode shown in Figure 3 was reduced from 19.68% to 5.50%, as evaluated by FESEM-EDS analysis. The Δj increment of the peak current intensity of the voltammograms in Figure 5 should actually be related to the widening of clean electrode areas achieved during regeneration.

If the voltammograms are traced for increasing upper potential value in the region of O_2 evolution, the electrode maintains an activity sufficient to continue the phenol oxidation owing to a sort of a continuous self-regeneration. However, oxygen evolution becomes the main electrochemical reaction at the anode and the current efficiency for phenol oxidation is significantly lowered. As outlined in earlier papers [2–4], bulk oxidants are also formed to enable parallel oxidation pathways. The nature of these oxidants depends on the potential reached and on the nature of the electrolyte. Table 1 lists the anode potentials needed to form the prevalent bulk oxidants [18].

As far as the nature of the electrolyte is concerned, the influence of chlorides is shown in Figure 6, where the results obtained during repeated voltammetric cycles are reported. The electrode loses activity during the first cycle but starting from the second cycle a new peak becomes visible. The intensity of this peak increases with the cycle number, along with the formation of chlorinated organic compounds. The run was repeated three times with good reproducibility. The presence of chlo-

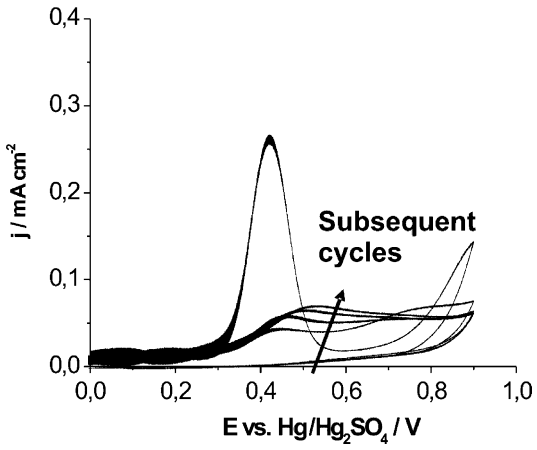

Fig. 6. Influence of the presence of chloride ions on phenol oxidation on the Pt anode. 5 mM of Phenol in 0.75 M Na_2SO_4 +0.25 M NaCl (initial potential = 0 V, sweep rate = 10 mV s^{-1}).

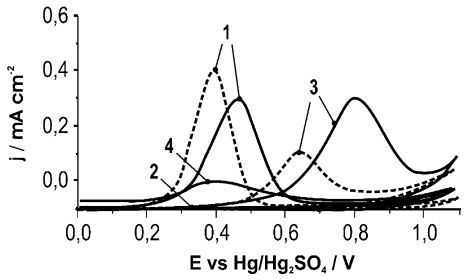

Fig. 7. Anodic part of voltammetric curves for phenol oxidation over the Pt electrode in clean state (1), after deactivation (2), and after reactivation for 15 min both at +1500 mV (3) and −800 mV (4). Experimental conditions: electrolyte: 0.2 M NaCl, T = 25 °C; initial potential = 0 V, sweep rate = 10 mV s^{-1}. Phenol concentration: [Ph] = 5 mM (solid lines); [Ph] = 50 mM (dashed lines).

rides seems to entails some self-regeneration of the electrodes in the mentioned operating conditions.

In order to clarify this issue, a regeneration test similar to the one related to Figure 4 (H_2SO_4 electrolyte) was accomplished, by using an aqueous solution containing only chlorides anions (0.2 M NaCl). As shown in Figure 7, the effectiveness of the electrode regeneration after treatment at +1500 mV is confirmed. However, displacement of the oxidation peak towards higher potential values can be noticed after the oxidative treatment (compare curves 1 and 3). This indicates a change in the nature of the active sites after regeneration, possibly linked to the formation of Pt–O or Pt–OH species. Moreover, phenol concentration was found to inhibit the formation of such oxidic species (compare dashed and full lines). It is likely that high Ph concentration cause high electrode surface coverage with phenol, thereby inhibiting the formation of Pt–OH species. This last effect is in line with the observations of other authors [19–23].

When reactivation is attempted during hydrogen evolution (−800 mV) the results are only slightly better than those obtained in Figure 4 for a sulphate containing electrolyte. The peak of the phenol oxidation after regeneration does not move from its original potential value. This is not surprising, since these last regeneration conditions are reducing and no oxidised Pt species should be formed over the electrode. This regeneration phenomenon is likely attributable to both the mechanical effect of gas bubble evolution and the partial reduction of organic material deposited.

Some further experiments were made in order to check the effect of the NaCl concentration on the regeneration at +1500 and +2200 mV. Figure 8 shows that the regeneration dynamics at +1500 mV in the presence of 0.2 M NaCl are faster than those encountered for a sulphate-based electrolyte (Figure 5). The regeneration occurring at +2200 mV is even faster, as a likely consequence of the generation of stronger and more numerous oxidative species. Since chlorides are present in most waste waters this issue should be of interest for practical applications. However, the regeneration dynamics are much slower when a NaCl concentration sufficiently low to enable direct discharge to water basins (0.02 M). This is a consequence of the lower current density, the electrode potential being the same.

Various galvanostatic tests were performed to detect the organic substances formed during phenol oxidation, in the absence and in the presence of chloride ions, at a current density of 10 mA cm^{-2}. The results obtained in a sulphate electrolyte containing 100 ppm of phenol after 4 h of electrolysis are summarised in Table 2, for Pt, Ti–Ir–Ta_2O_5 and PbO_2 electrodes.

The remarkable difference in the phenol concentrations can be ascribed to processes occurring in the electrolyte which depend on the H_2O_2 production. Indirect oxidation routes promoted by the Pt electrode seem to lead to higher phenol degradation, but also to the formation of significant quantities of benzo- and hydro-quinone. Conversely, the other two electrodes mainly cause direct anodic oxidation which ends up in complete oxidation to CO_2 and limited formation of intermediates.

When operating in the presence of a Cl^- containing electrolyte with the Pt electrode, deleterious amounts of small-molecular-size chlorinated hydrocarbons were generated (Figure 9). The chlorinated compounds are not biodegradable and might have a tendency to leave the solution, being released in the atmosphere where they can act as ozone-damaging gases. This hampers the

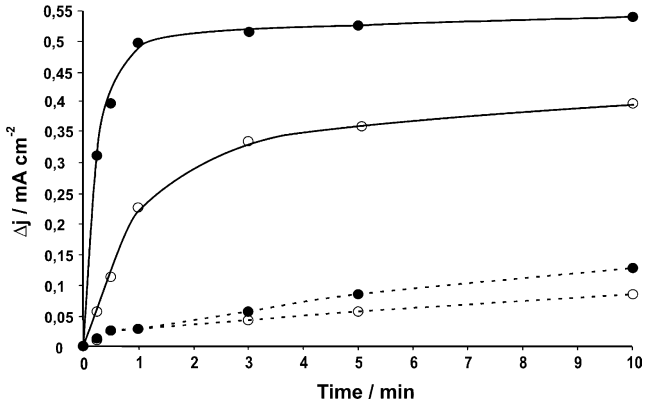

Fig. 8. Influence of regeneration time at both +1500 mV (○) and +2200 mV (●) on the recovered oxidation peak intensity for 5 mM phenol in 0.2 M NaCl (solid lines) or 0.02 M NaCl (dashed lines) solution over a Pt anode (initial potential = 0 V, sweep rate = 10 mV s^{-1}).

Table 2. Molar concentrations of reaction intermediates measured after 4 h of electrolysis with the various electrodes tested (initial phenol concentration = 100 ppm, i = 10 mA cm^{-2}, electrolyte = sodium sulphate)

Concentration (ppm)	Pt	PbO_2	Ti/IrO_2/Ta_2O_5
Phenol	35	60	70
Benzoquinone	9	0	0
Hydroquinone	57	6	8
Cathecol	2.5	0	0

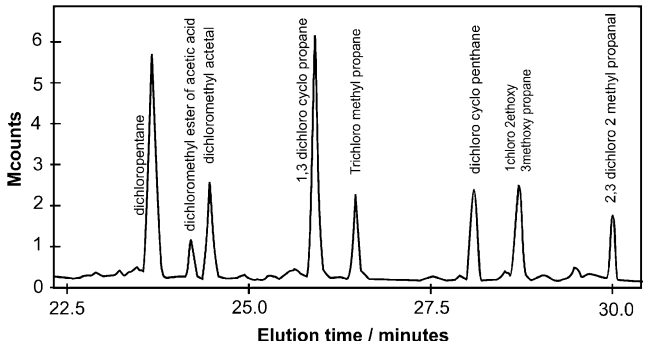

Fig. 9. Chromatographic analysis results showing the chlorinated compounds generated after 4 h of phenol electro-oxidation over the Pt anode (initial phenol concentration = 100 ppm, i = 10 mA cm^{-2}, electrolyte = 0.75 M Na_2SO_4 + 0.25 M NaCl).

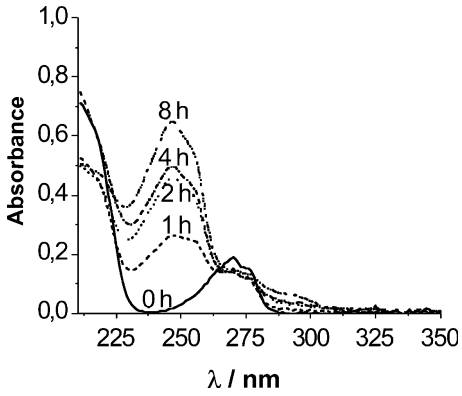

Fig. 11. UV spectra for various samples withdrawn periodically from the electrolyte H_2SO_4 0.5 M. Initial [Ph] = 5 mM; electrode = activated carbon; I = 0.1 mA/g of C.

achievement of complete organic compound abatement. Since the amount of electrode surface deactivating species is reduced (see Figure 6–8 above), it might be hypothesised that some of these chlorinated compounds might be generated from such deactivating polymeric species.

Regarding the deactivation/regeneration behaviour of the $Ti/IrO_2/Ta_2O_5$ electrode, the voltammetric analyses showed that after the first cycle the anode remains in the deactivated state even though a high positive potential is applied. The potential necessary for the reactivation requires too high current intensities for practical use. This electrode is actually designed to allow oxygen evolution at low potential values. As a consequence, no formation of highly oxidising species (e.g. OH° takes place to enable regeneration. Conversely, cyclic voltammetric curves on PbO_2 electrodes are not reported because the intensity of the lead-dioxide reduction peak is so high that the peaks for phenol oxidation are hardly detected.

As far as the performance of the carbon electrode is concerned, phenol is rapidly adsorbed on the active carbon. For this reason the tests were made with carbon previously saturated with phenol at ambient temperature (0.230 mg of Ph(mg of C)$^{-1}$). After anodic polarisation in sulphate media the organic compound released in the electrolyte is benzoquinone (Figure 10). In this Figure, the amount of phenol, which at the same time is desorbed from the carbon, is also reported.

Finally, the UV spectra determined during the anodic oxidation of phenol over the carbon electrode obtained without and with chloride are reported in Figures 11 and 12, respectively. When the chlorides are absent, the phenol abatement is comparatively slower and a new peak, increasing with time, appears in the spectra. This peak is attributable to benzoquinone and/or hydroquinone generation. This secondary peak is almost absent when operating with the chloride-containing electrolyte. This is an indication that the latter electrolyte promotes ClO^- formation which, in turn, enables a faster oxidation of phenol as well as of its prevalent reaction intermediates (benzo-/hydro-quinone). HPLC analyses confirmed this deduction, showing the presence of a number of chlorinated hydrocarbons in the solution corresponding to the peak observed after 24 h of treatment at a wavelength of about 300 nm (Figure 12). Such compounds are nearly the same ones shown in

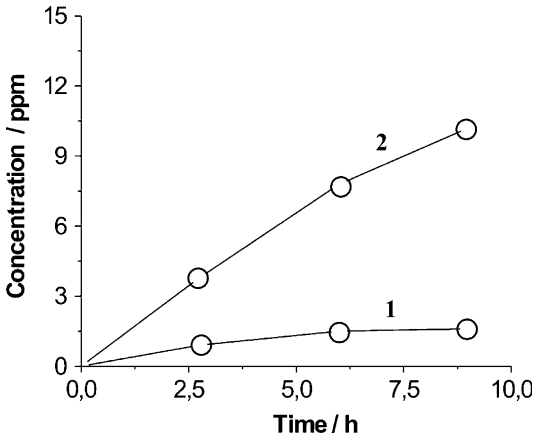

Fig. 10. Curve 1: BQ generation from phenol degradation on the Ph-saturated C electrode at I = 0.1 mA/g of C in Na_2SO_4 0.025 M. Curve 2: Ph desorbed from the carbon at the same time.

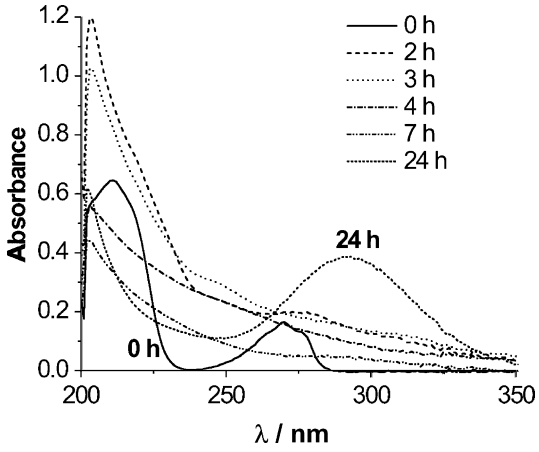

Fig. 12. UV spectra for various samples withdrawn periodically from the electrolyte. [Ph] = 5 mM; electrolyte = 0.75 Na_2SO_4 + 0.25 M NaCl; electrode = activated carbon; I = 0.1 mA/g of C.

Figure 7, with minor differences in the relative chromatographic peak intensities.

4. Conclusions

The oxidation of phenol on various anodes has been investigated mainly by means of voltammetric tests, which showed that, in the absence of chloride ions, the electrode remains deactivated if the upper potential value is lower than 1300 mV vs Hg/Hg_2SO_4, while it can be reactivated if the potential goes up to 1500 mV vs Hg/Hg_2SO_4.

When chloride ions are present, the Pt electrode loses activity during the first cycle, but on continued cycling a new anodic peak appears, whose intensity increases along with the formation of chlorinated organic compounds. Specific experiments carried out on solutions containing only NaCl as electrolyte showed that regeneration at +1500 mV occurs at a much faster rate than in the case of sulphate-based electrolytes, at the price of the formation of a series of potentially harmful chlorinated hydrocarbons.

Comparison of the different anodes showed that with PbO_2 and $Ti/IrO_2/Ta_2O_5$ electrodes the direct electrooxidation prevails against the indirect chemical oxidation. With these electrodes lower degradation of phenol is obtained compared to the Pt anode, but they produce a low quantity of intermediates. Similar effects are observed with carbon electrodes, for which the presence of chloride ions seems to promote a faster oxidation of phenol, thus producing less benzo-/hydro-quinone intermediates.

Since the presence of H_2O_2 directly influences the chemical oxidation of the organic substances, a cell for practical application could employ gas diffusion electrodes for the cathodic production of hydrogen peroxide. Other possible solutions for phenolic compound oxidation, based on regenerative cells, do not appear easily applicable due to the high anodic potential required for the reactivation of the electrode surface.

References

1. M. Maja, G. Saracco and V. Specchia, 'Electrochemical Oxidation of Wastewater Containing Coumaric Acid', 48th Meeting of ISE, Paris 1997. Book of Abstracts, p. 758.
2. G. Saracco, L. Solarino, R. Aigotti, V. Specchia and M. Maja, *Electrochim. Acta* **46** (2000) 373.
3. G. Saracco, R. Aigotti, L. Solarino, V. Specchia and M. Maja, *Ann. Chim.* **91** (2001) 211.
4. G. Saracco, L. Solarino, V. Specchia and M. Maja, *Chem. Eng. Sci.* **56** (2001) 1571.
5. M. Gattrell and D.W. Kirk, *J. Electrochem. Soc* **140** (1993) 1534.
6. R.C. Koile and D.C. Johnson, *Anal. Chem* **51** (1979) 741.
7. B. Fleszar and J. Ptoszynska, *Electrochim. Acta* **30** (1985) 31.
8. J.L. Boudenne, O. Cerclier and P. Bianco, *J. Electrochem. Soc* **145** (1998) 2763.
9. Ch. Comminellis and C Pulgarin, *J. App. Electrochem* **21** (1991) 703.
10. J. Iniesta, E. Exposito, J. Gonzales-Garcia, V. Montiel A. Aldaz, *J. Electrochem. Soc* **149** (2002) D57.
11. P. Canizares, F. Martinez, M. Diaz, J. Garcia-Gomez and M.-A. Rodrigo, *J. Electrochem. Soc* **149** (2002) D118.
12. Ch. Comminellis and A. Nerini, *J. App. Electrochem* **25** (1995) 23.
13. C. Borra, A. Di Corcia, M. Marchetti and R. Samperio, *Anal. Chem* **58** (1986) 2048 .
14. B.E. Hayden, D.V. Malevich and D. Pletcher, *Electrochem. Comun* **3** (2001) 396.
15. S. Andreescu, D. Andreescu and O.A. Sadik, *Electrochem. Comun* **5** (2003) 681.
16. 16. M.W. Breither, 'Electrochemical Processes in Fuel Cells' (Elsevier, 1969).
17. NIST spectra database, http://webbook.nist.gov.
18. I. Tröster, M. Fryda, D. Herrmann, L. Schafer, W. Hanni A. Perret, M. Blaschke, A. Kraft and M. Stadelmannc, *Diamond Rel. Mat* **11** (2002) 643.
19. Y. Yang and G. Denuault, *J. Electroanal. Chem* **443** (1998) 273.
20. P.I. Iotov and S.V. Kalcheva, *J. Electroanal. Chem* **442** (1998) 19.
21. H. Kuramitz, Y. Nakata, M. Kawasaki and S. Tanaka, *Chemosphere* **45** (2001) 37.
22. C. Hu and K. Liu, *Electrochim. Acta* **44** (1999) 2727.
23. B.E. Conway. *in* S. Trasatti (Ed), Electrodes of Conductive Metallic Oxides, Part B (Elsevier, New York, 1981).